Time lags and reverberation in the lamp-post geometry of the compact corona illuminating a black-hole accretion disc

Michal Dovčiak

Astronomical Institute
Academy of Sciences of the Czech Republic, Prague

Astrophysics group seminar, School of Physics, University of Bristol

13th March 2014

Acknowledgement

StrongGravity (2013–1017) — EU research project funded under the Space theme of the 7th Framework Programme on Cooperation

Title: **Probing Strong Gravity by Black Holes Across the Range of Masses**

Institutes: AsU, CNRS, UNIROMA3, UCAM, CSIC, UCO, CAMK

Webpages: `http://stronggravity.eu/`

`http://cordis.europa.eu/projects/rcn/106556_en.html`

Active Galactic Nuclei – scheme

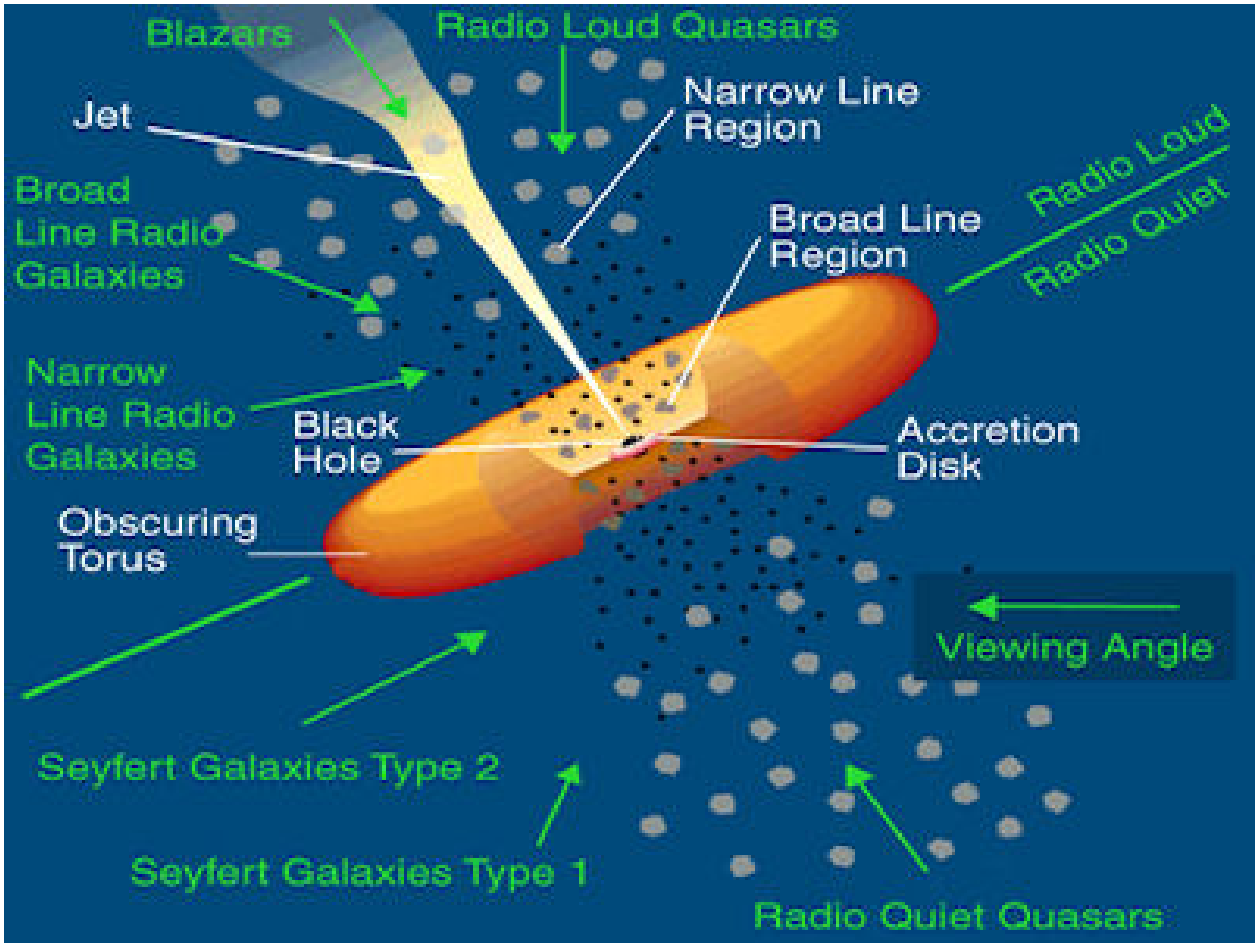

Urry C. M. & Padovani P. (1995)
Unified Schemes for Radio-Loud Active Galactic Nuclei
PASP, 107, 803

Active Galactic Nuclei – X-ray spectrum

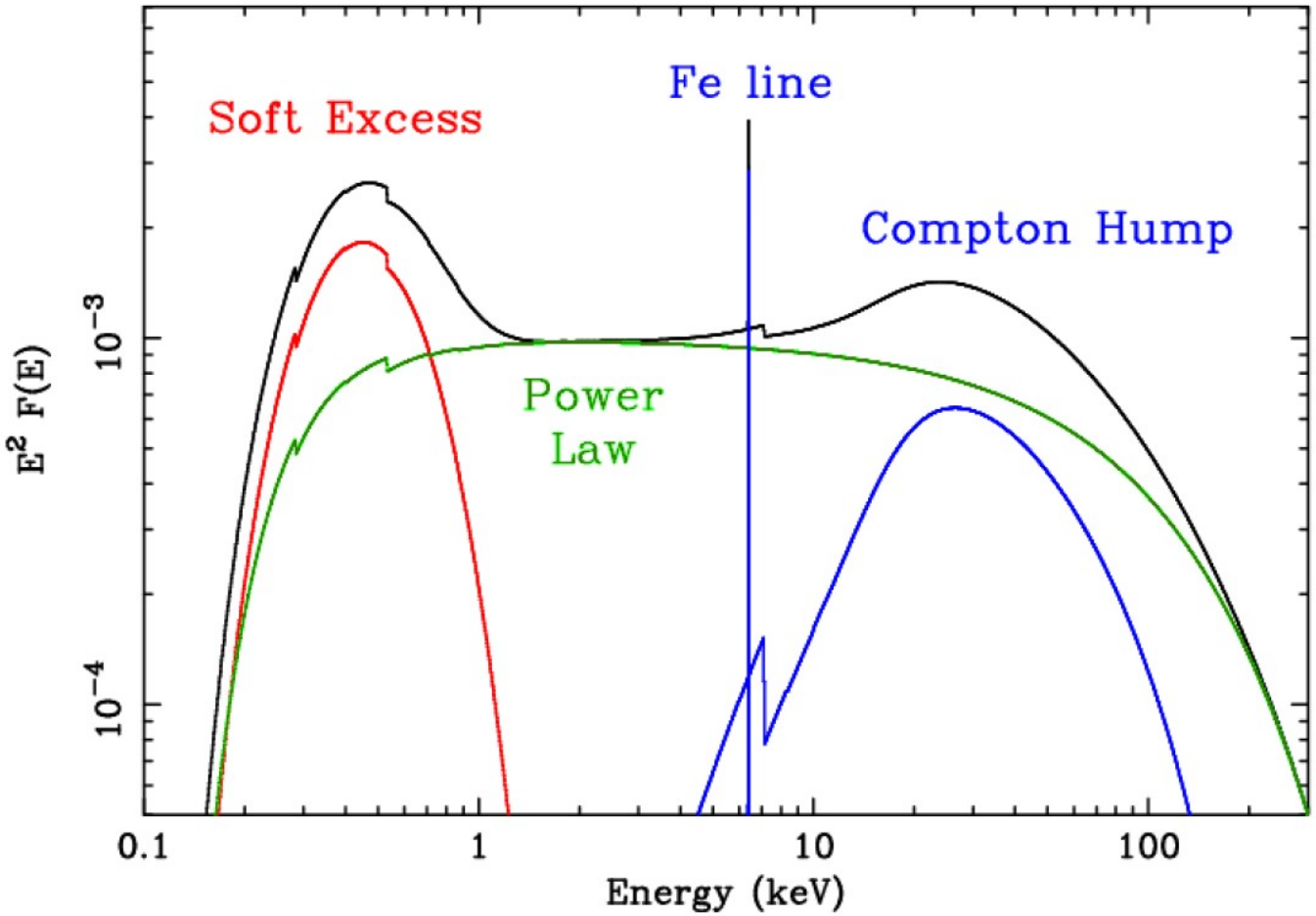

Fabian A.C. (2005)
X-ray Reflections on AGN,
in proceedings of “The X-ray Universe 2005”, El Escorial, Madrid, Spain, 26-30/9/2005

References

- Blandford & McKee (1982) ApJ **255** 419 $\rightarrow$ reverberation of BLR

$$L_{\rm o}(v,t) = \int_{-\infty}^{\infty} dt'\, L_{\rm p}(t')\, \Psi(v, t-t')$$

- Stella (1990) Nature **344** 747 $\rightarrow$ time dependent Fe Kα shape ($a = 0$)
- Matt & Perola (1992) MNRAS **259** 433
  $\rightarrow$ Fe Kα response and black hole mass estimate $\rightarrow t \sim GM/c^3$
  $\rightarrow$ time dependent light curve, centroid energy and line equivalent width ($h = 6, 10$; $a = 0$; $\theta_{\rm o}$)
- Campana & Stella (1995) MNRAS **272** 585
  $\rightarrow$ line reverberation for a compact and extended source ($a = 0$)
- Reynolds, Young, Begelman & Fabian (1999) ApJ **514** 164
  $\rightarrow$ fully relativistic line reverberation ($h = 10$; $a = 0, 1$)
  $\rightarrow$ more detailed reprocessing, off-axis flares
  $\rightarrow$ ionized lines for Schwarzschild case, outward and inward echo, reappearance of the broad relativistic line

References

- Wilkins & Fabian (2013) MNRAS **430** 247

  $\rightarrow$ fully relativistic, extended corona, propagation effects
- Cackett et al. (2014) MNRAS **438** 2980

  $\rightarrow$ Fe Kα reverberation in lamp-post model

Scheme of the lamp-post geometry

- central black hole – mass, spin
- compact corona with isotropic emission
  → height, photon index
- accretion disc
  → Keplerian, geometrically thin, optically thick
  → ionisation due to illumination
  (L_p, h, M, a, n_H, q_n)
- local re-processing in the disc
  → REFLIONX with different directional emissivity prescriptions
- relativistic effects:
  → Doppler and gravitational energy shift
  → light bending (lensing)
  → aberration (beaming)
  → light travel time

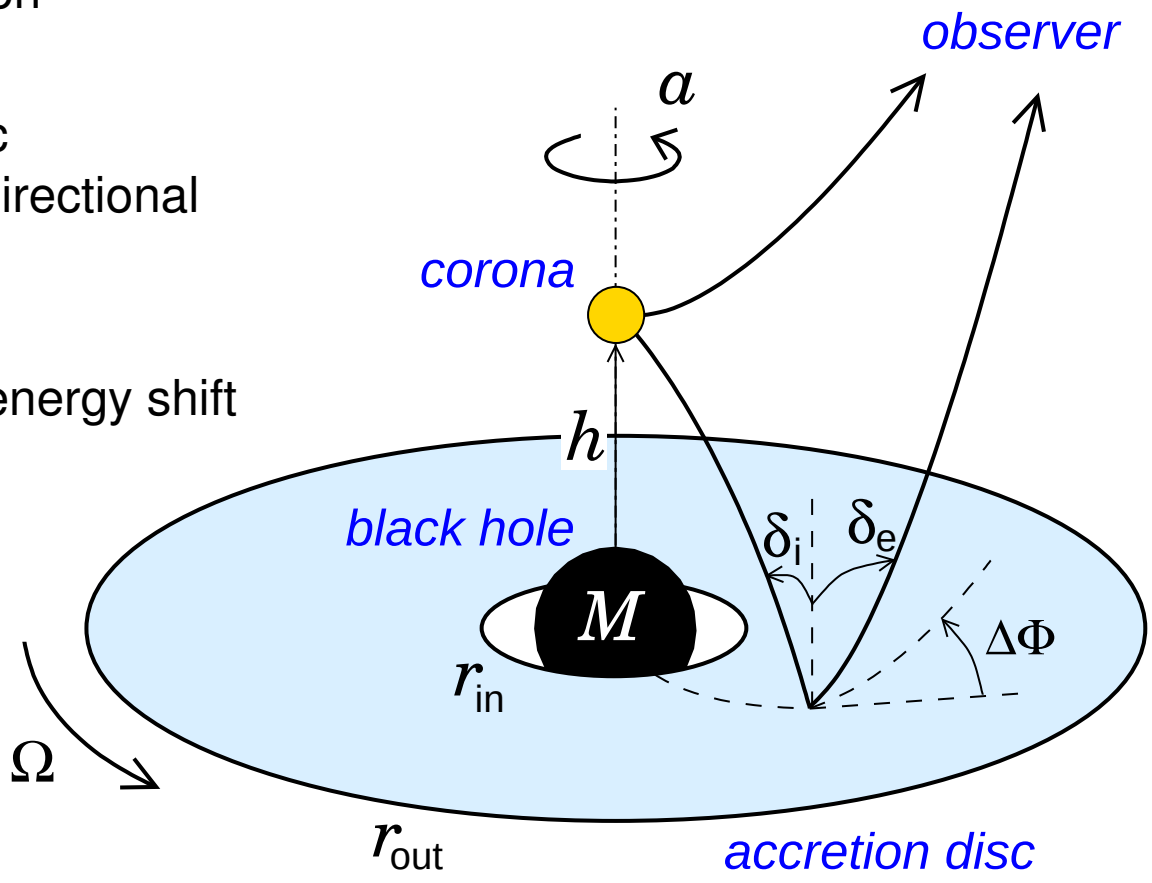

Time delay

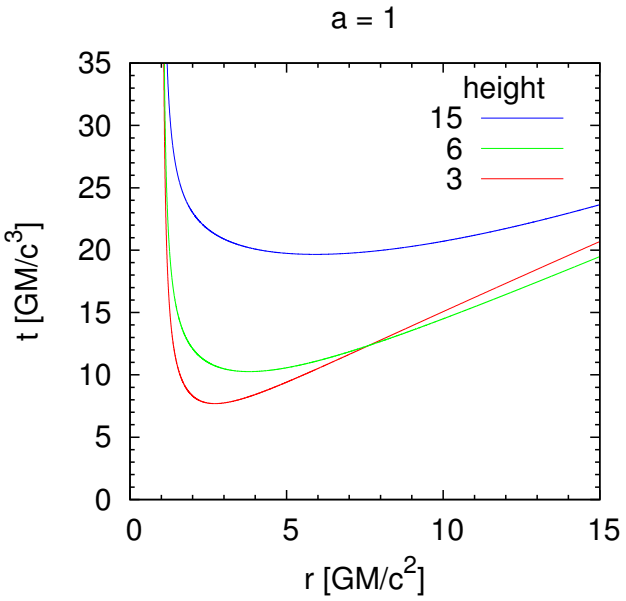

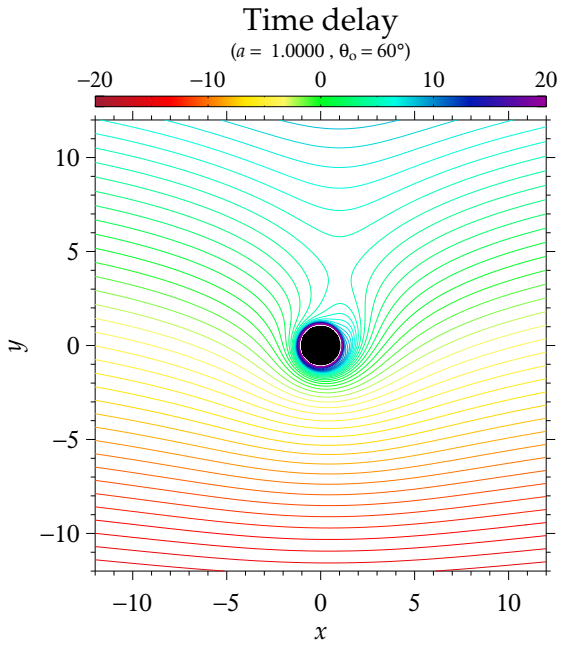

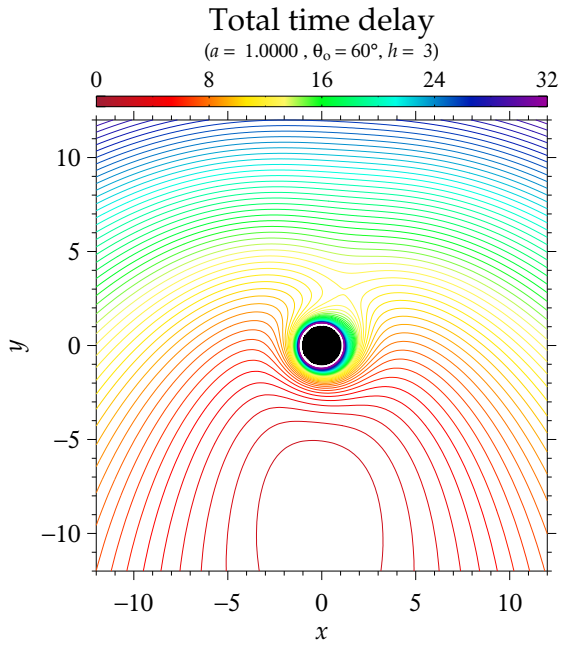

- total light travel time includes the lamp-to-disc and disc-to-observer part
- first photons arrive from the region in front of the black hole which is further out for higher source
- contours of the total time delay shows the ring of reflection that develops into two rings when the echo reaches the vicinity of the black hole

Light curve

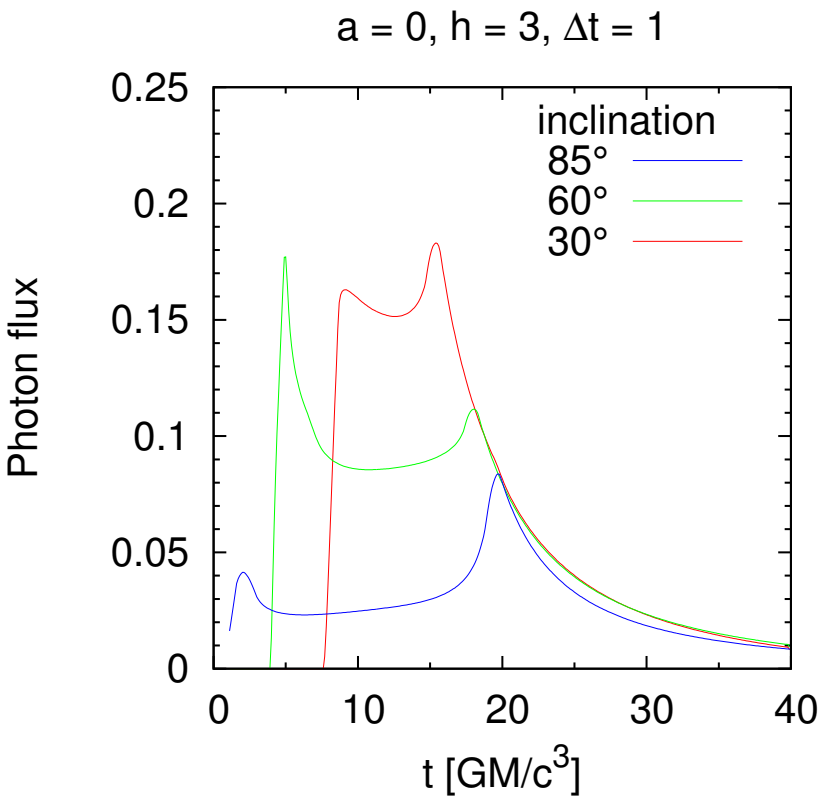

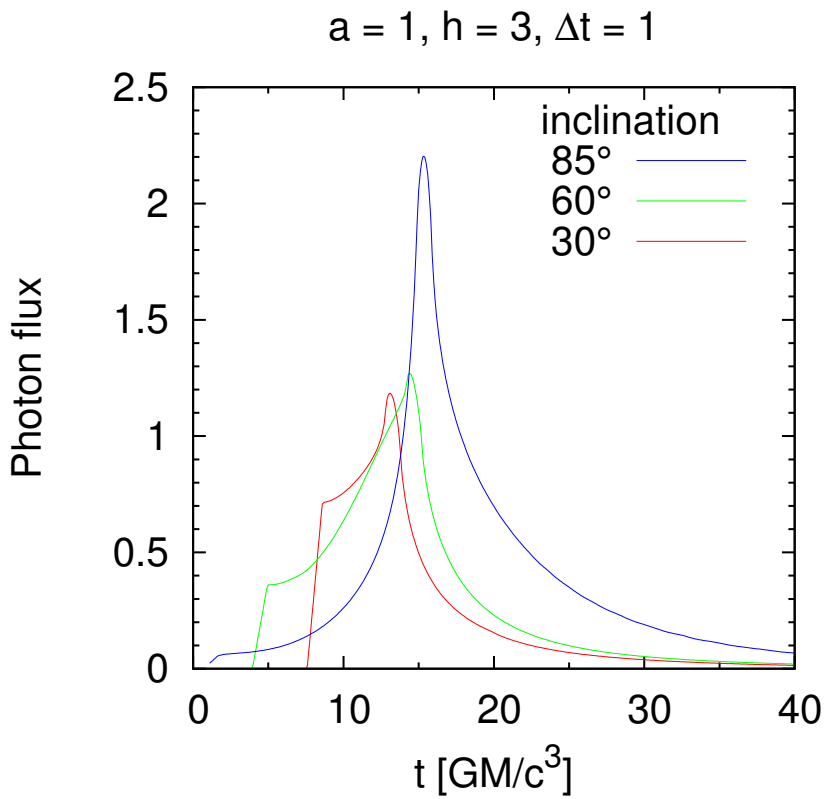

- the flux for Schwarzschild BH is much smaller than for Kerr BH due to the hole below ISCO (no inner ring in Schwarzschild case)
- the shape of the light curve differs substantially for different spins
- the “duration” of the echo is quite similar
- the higher the inclination the sooner first photons will be observed
- magnification due to lensing effect at high inclinations

Dynamic spectrum

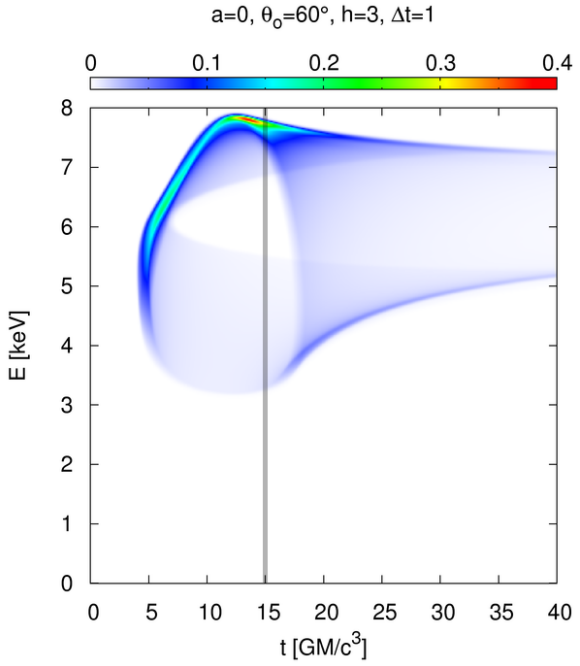

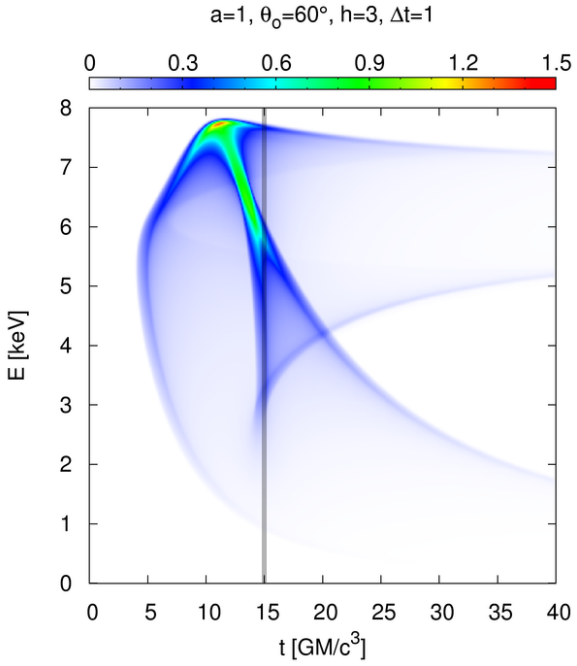

- signature of outer and inner echo in dynamic spectra
- large amplification when the two echos separate
- intrinsically narrow Kα line can acquire weird shapes

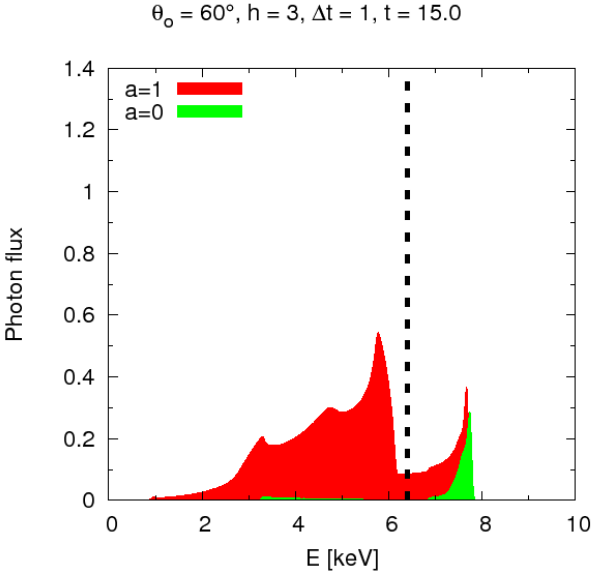

Transfer function for reverberation

Stationary emission from the accretion disc:

$$F(E) = \int r\,dr\,d\varphi\,G(r,\varphi)\,F_{\rm I}(r,\varphi,E/g)$$

Response to the on-axis primary emission:

$$F(E,t) = \int dt' \int r\,dr\,d\varphi\,G(r,\varphi)\times$$
$$N_{\rm p}(t')\,N_{\rm inc}(r)\,M(r,\varphi,E/g,t'+t_{\rm pd})\,\delta([t-t_{\rm do}]-[t'+t_{\rm pd}])$$

Line reverberation:

$$F(E,t) = \int dt'\,N_{\rm p}(t') \int r\,dr\,d\varphi\,\Psi_0(r,\varphi)\,\delta(E-gE_{\rm rest})\,\delta([t-t']-\underbrace{[t_{\rm pd}+t_{\rm do}]}_{\Delta t})$$

$$G = g\,\mu_{\rm e}\,\ell$$
$$g = \frac{E}{E_{\rm I}}$$
$$\mu_{\rm e} = \cos\delta_{\rm e}$$
$$\ell = \frac{dS_{\rm o}}{dS_{\rm I}^{\perp}}$$
$$N_{\rm inc} = g_{\rm inc}^{\Gamma}\,\frac{d\Omega_{\rm p}}{dS_{\rm inc}}$$
$$\Psi_0 = g\,G\,N_{\rm inc}\,M$$

Transfer function $\rightarrow$ response to a flare [$N_{\rm p}(t') = \delta(t')$]:

$$\Psi(E,t) = \sum_{\substack{g=E/E_{\rm rest}\\ t_{\rm pd}+t_{\rm do}=t}} \Psi_0\,\frac{r}{E_{\rm rest}}\left|\frac{\partial(g,\Delta t)}{\partial(r,\varphi)}\right|^{-1}$$

$$F(E,t) = \int dt'\,N_{\rm p}(t')\,\Psi(E,t-t')$$

$$\frac{\partial(g,\Delta t)}{\partial(r,\varphi)} = \frac{\partial g}{\partial r}\frac{\partial(\Delta t)}{\partial\varphi} - \frac{\partial g}{\partial\varphi}\frac{\partial(\Delta t)}{\partial r} \neq 0 \qquad \Rightarrow \qquad \nabla g \nparallel \nabla(\Delta t)$$

Caustics – Schwarzschild case

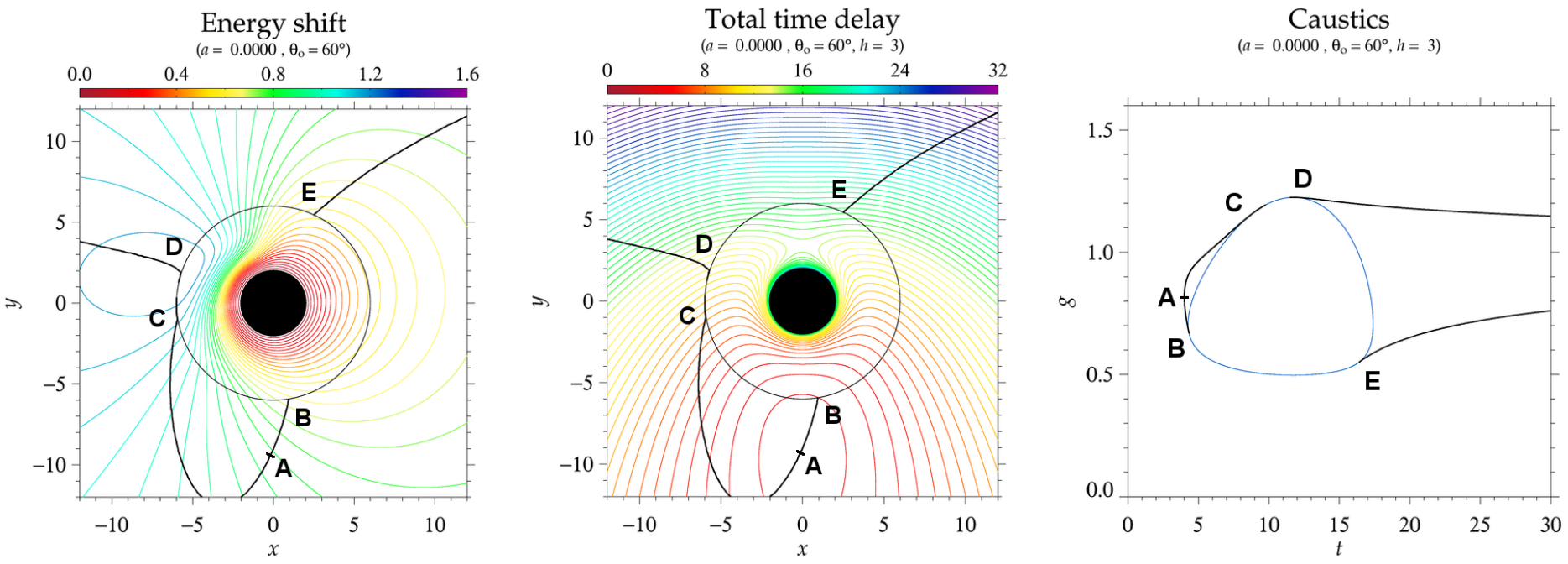

- the black curves show the points where the energy shift contours are tangent to the time delay ones
- contour of ISCO in energy-time plane is shown by the blue curve
- the correspondent points A, B, C, D and E are shown in each plot for better understanding

Caustics – extreme Kerr case

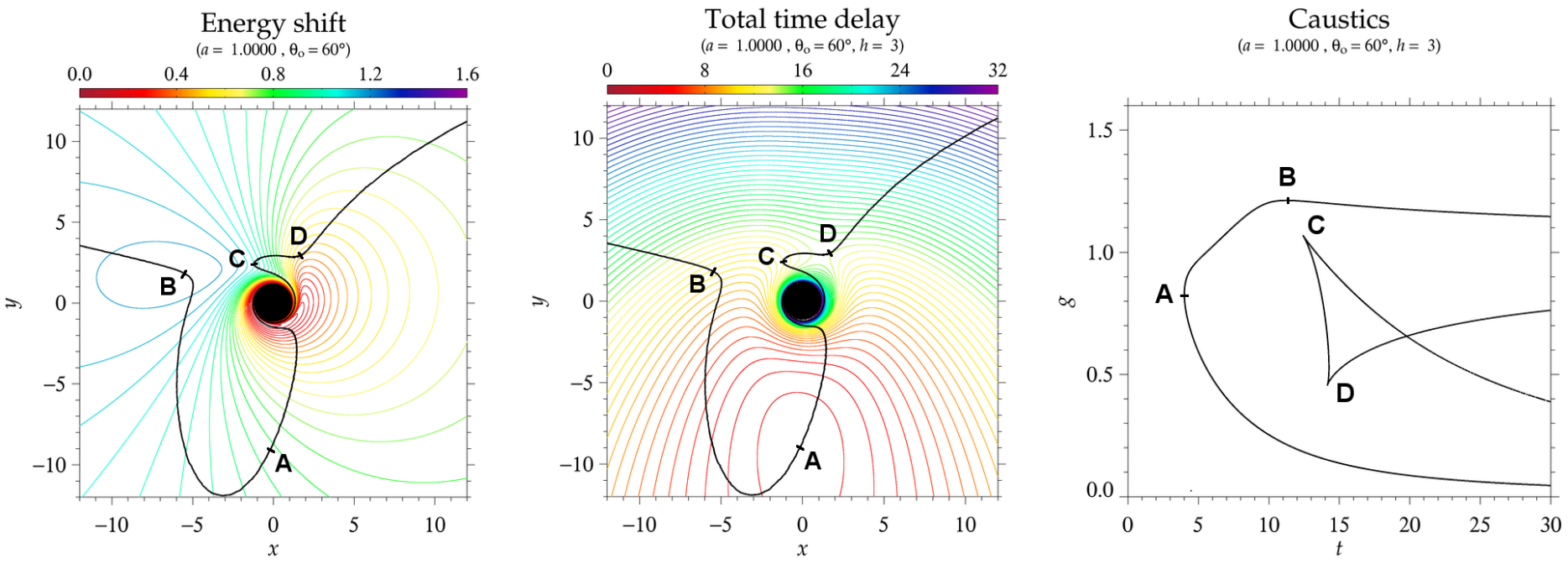

- the black curves show the points where the energy shift contours are tangent to the time delay ones
- contour of ISCO in energy-time plane is shown by the blue curve
- the correspondent points A, B, C, D and E are shown in each plot for better understanding

Caustics

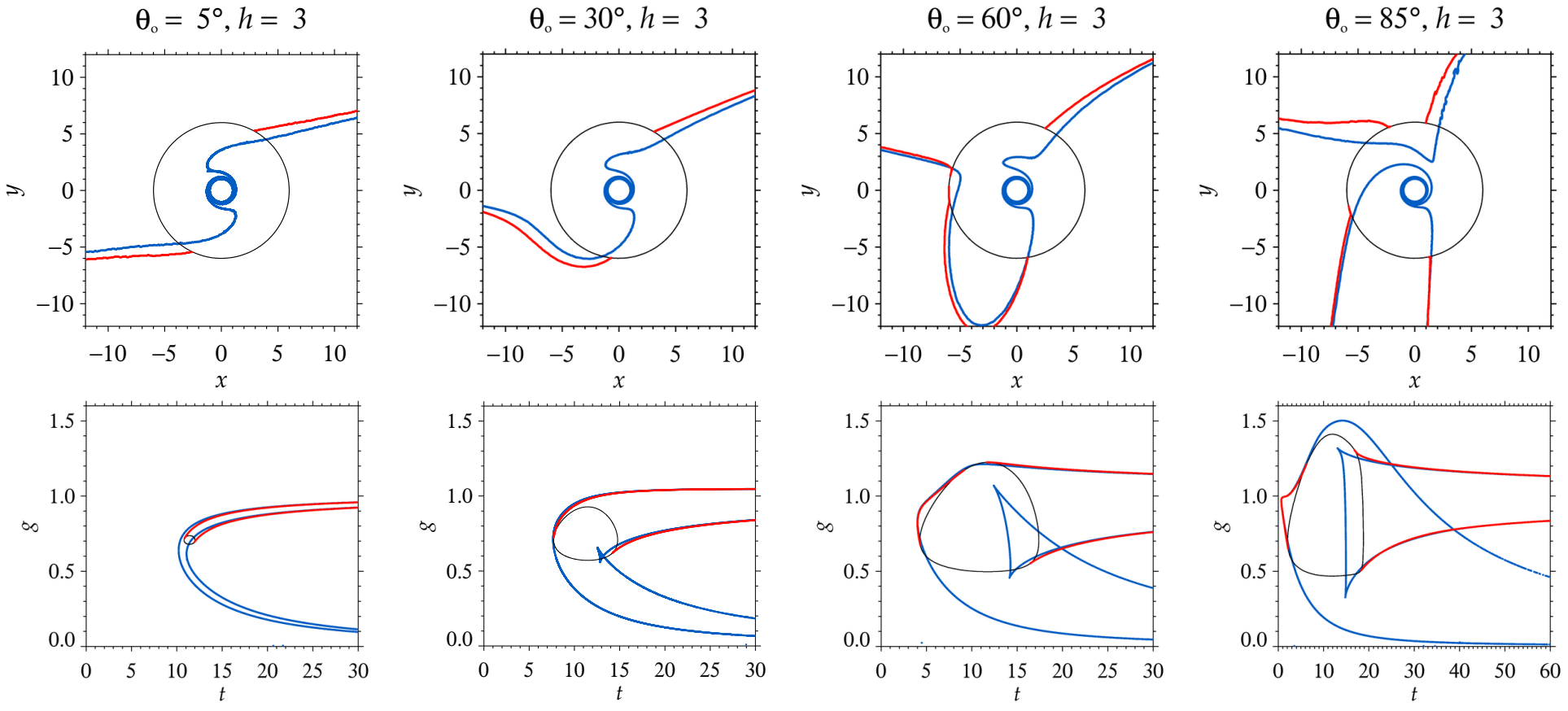

- plots of infinite magnification in the x-y (top) and g-t (bottom) planes
- the plots for Schwarzschild case (red) above ISCO are very similar to the extreme Kerr case (blue)
- the shape of these regions change with inclination

Dynamic spectrum – narrow spectral line

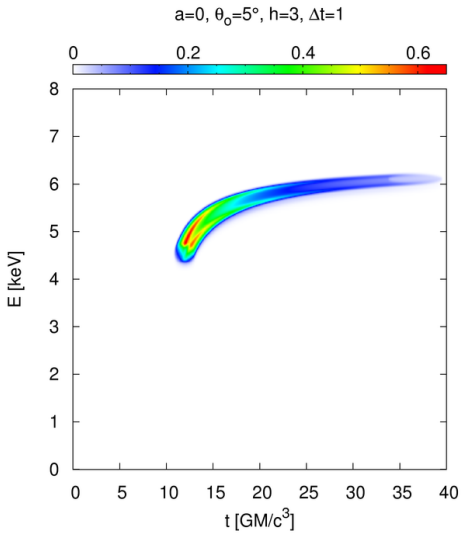

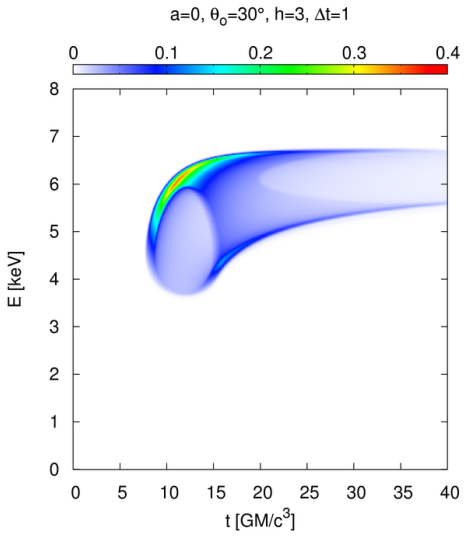

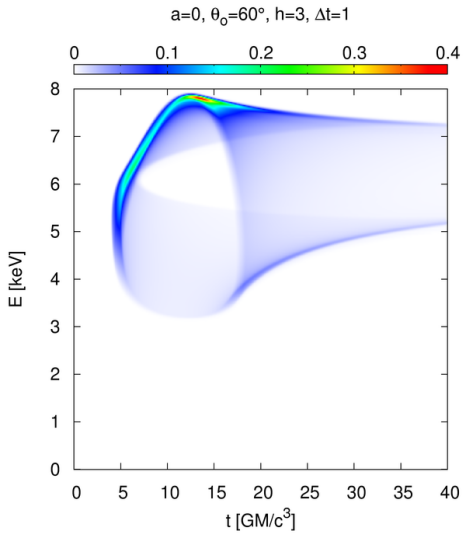

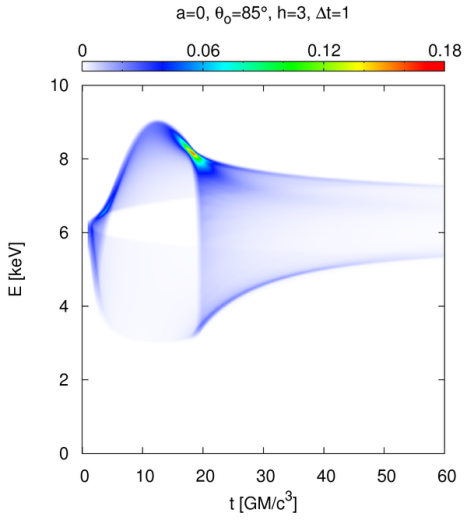

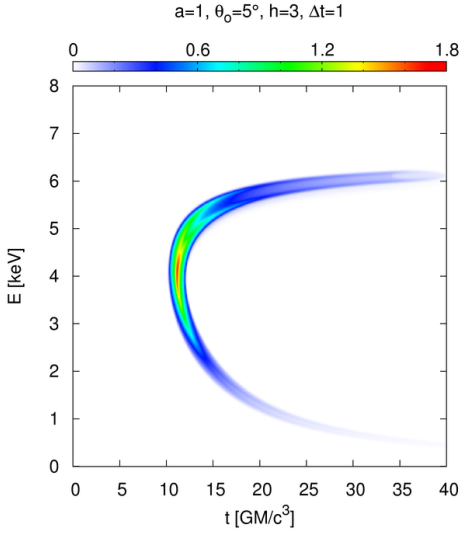

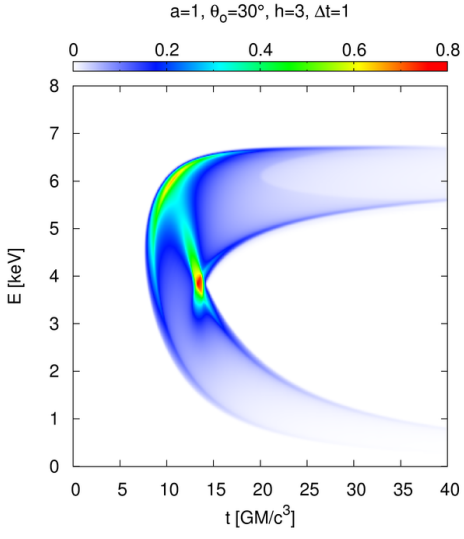

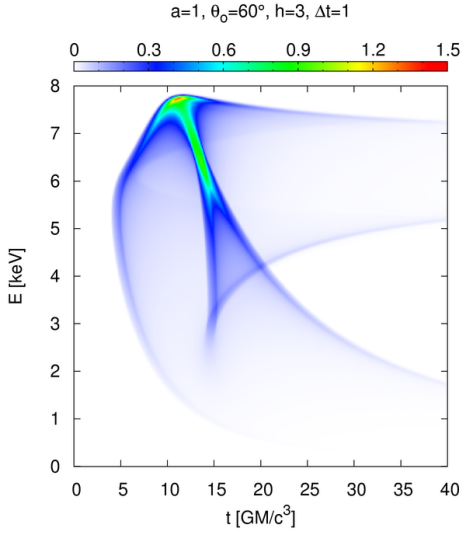

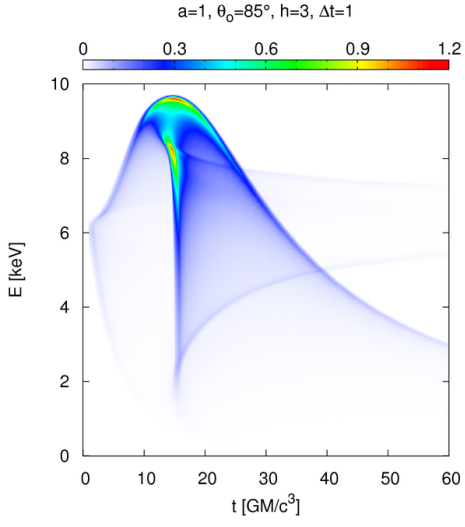

Dynamic spectrum – neutral disc

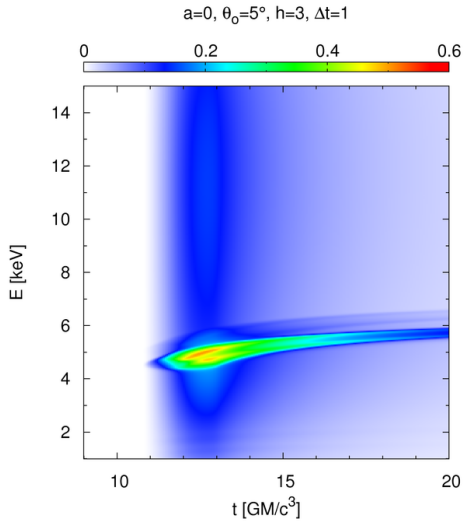

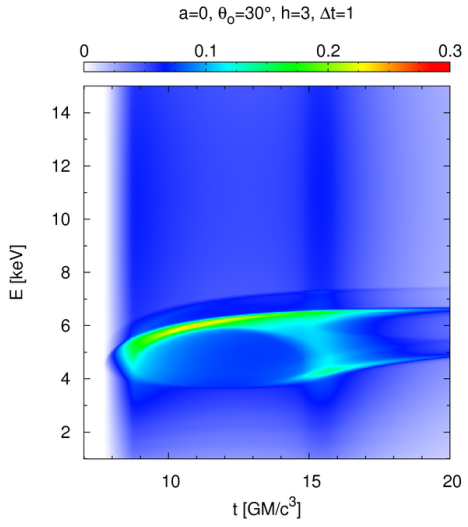

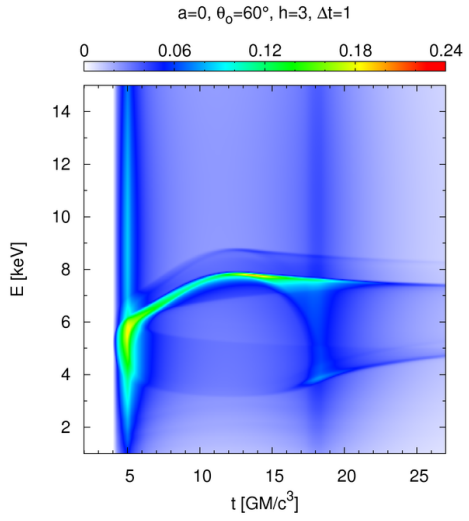

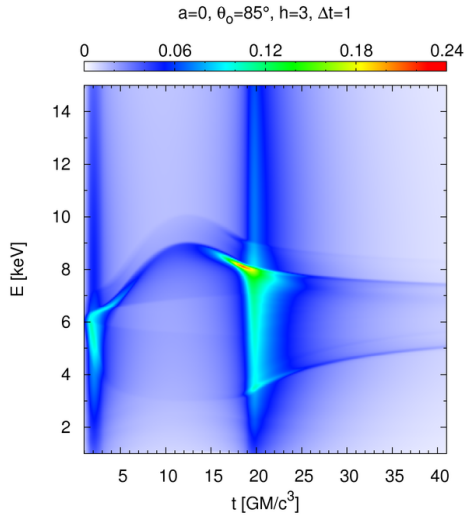

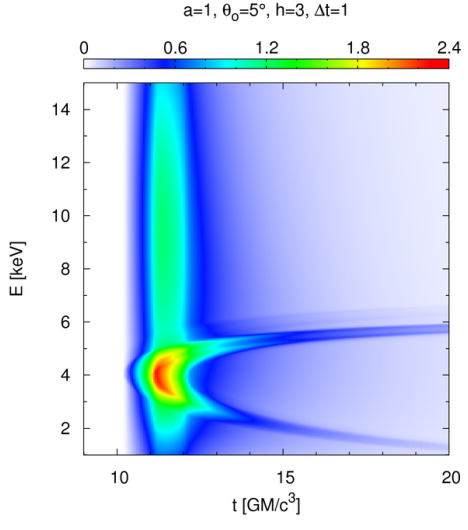

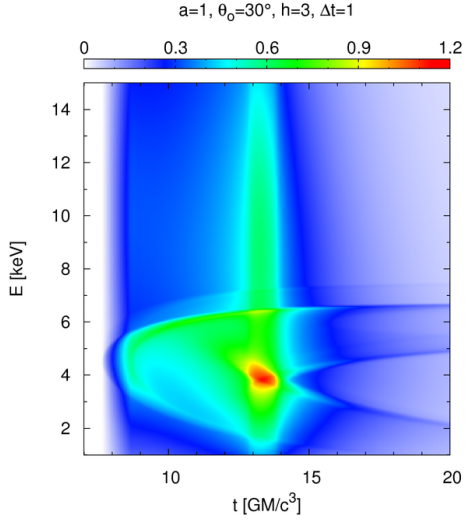

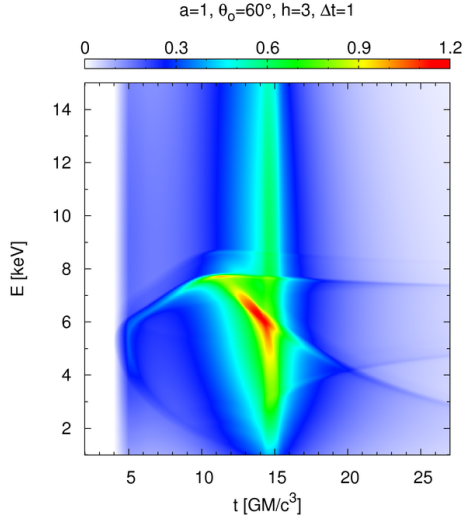

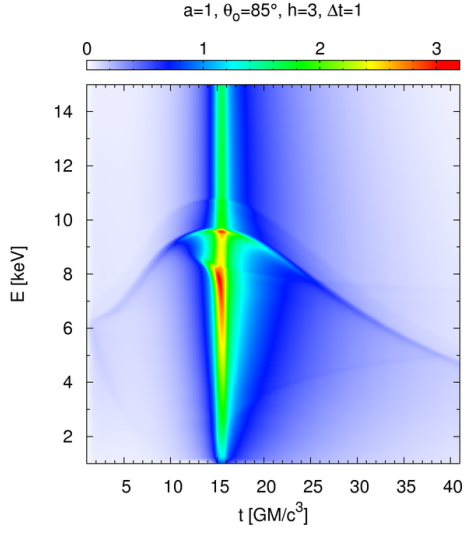

Dynamic spectrum – ionised disc

$$E^2 \times F(E)$$

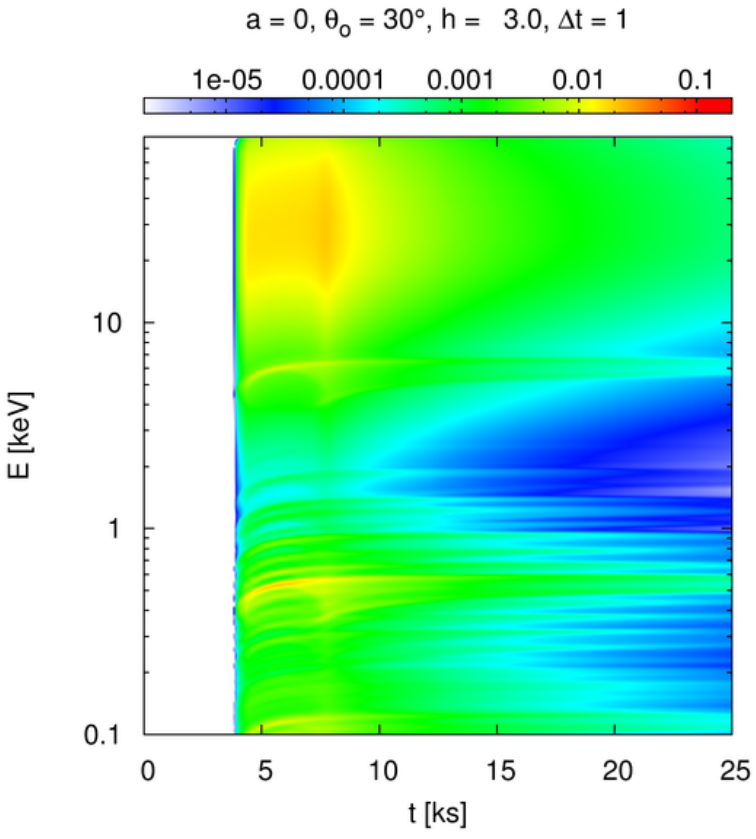

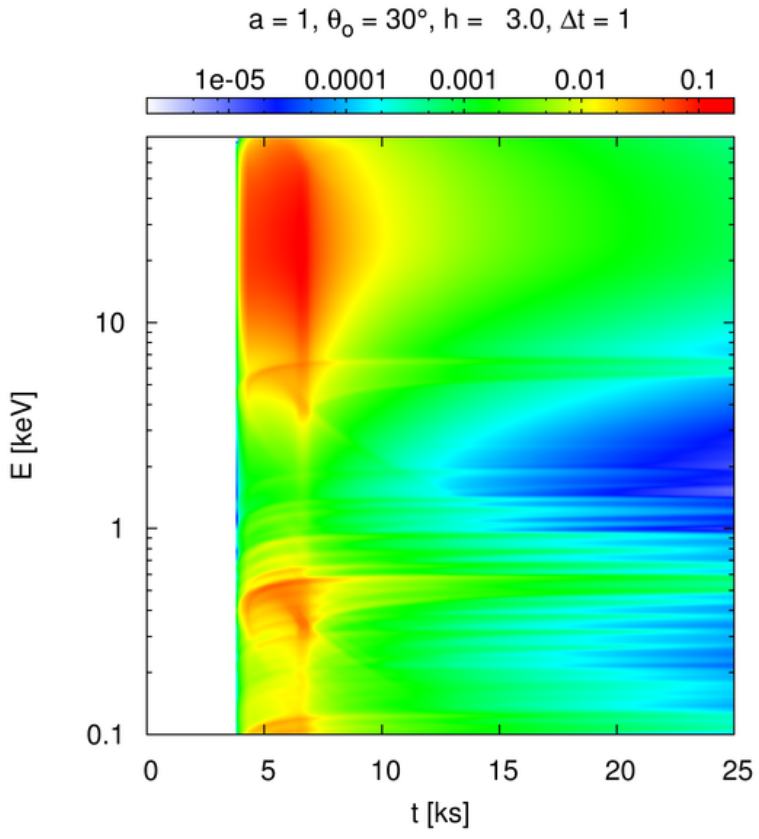

Definition of the phase lag

$$F_{\mathrm{refl}}(E,t) = N_{\mathrm{p}}(t) * \psi(E,t) \qquad \Rightarrow \qquad \hat{F}_{\mathrm{refl}}(E,f) = \hat{N}_{\mathrm{p}}(f).\hat{\psi}(E,f)$$

where

$$\hat{\psi}(E,f) = A(E,f)e^{i\phi(E,f)}$$

---

if

$$N_{\mathrm{p}}(t) = \cos(2\pi f t) \qquad \text{and} \qquad \hat{\psi}(\mathrm{E}) = \mathrm{A(E)e}^{\mathrm{i}\phi(\mathrm{E})}$$

then

$$F_{\mathrm{refl}}(E,t) = A(E)\cos\{2\pi f[t+\tau(E)]\} \qquad \text{where} \qquad \tau(\mathrm{E}) \equiv \frac{\phi(\mathrm{E})}{2\pi \mathrm{f}}$$

$$F(E,t) \sim N_{\mathrm{p}}(t) * (\psi_{\mathrm{r}}(E,t) + \delta(t)) \qquad \Rightarrow \qquad \hat{F}(E,f) \sim \hat{N}_{\mathrm{p}}(f).(\hat{\psi}_{\mathrm{r}}(E,f) + 1)$$

and

$$\tan\phi_{\mathrm{tot}}(E,f) = \frac{A_{\mathrm{r}}(E,f)\sin\phi_{\mathrm{r}}(E,f)}{1 + A_{\mathrm{r}}(E,f)\cos\phi_{\mathrm{r}}(E,f)}$$

Parameter values and integrated spectrum

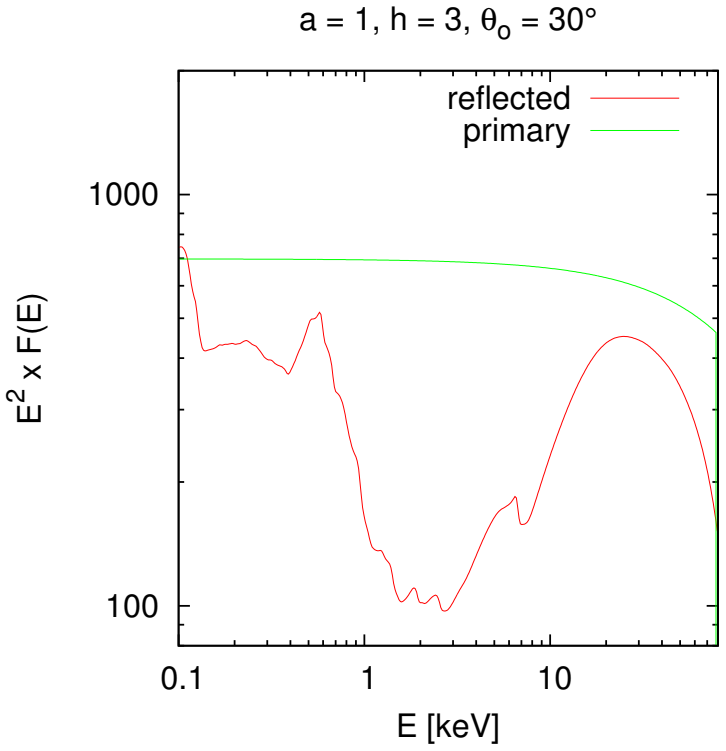

$$
\begin{aligned}
M &= 10^8 M_\odot \\
a &= 1\ (0) \\
\theta_o &= 30^\circ\ (60^\circ) \\
h &= 3\ (1.5,\ 6,\ 15,\ 30) \\
L_p &= 0.001\, L_{\mathrm{Edd}} \\
\Gamma &= 2\ (1.5,\ 3) \\
n_H &= 0.1\ (0.01,\ 50,\ 5,\ 0.2) \times 10^{15}\mathrm{cm}^{-3} \\
q_n &= -2\ (0,\ -5,\ -3)
\end{aligned}
$$

Energy bands: soft excess: $0.3 - 0.8$ keV

primary: $1 - 3$ keV

iron line: $3 - 9$ keV

Compton hump: $15 - 40$ keV

Phase lag dependence on geometry

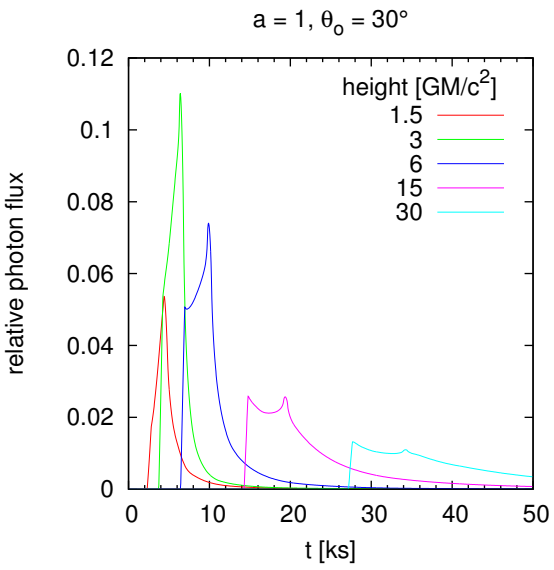

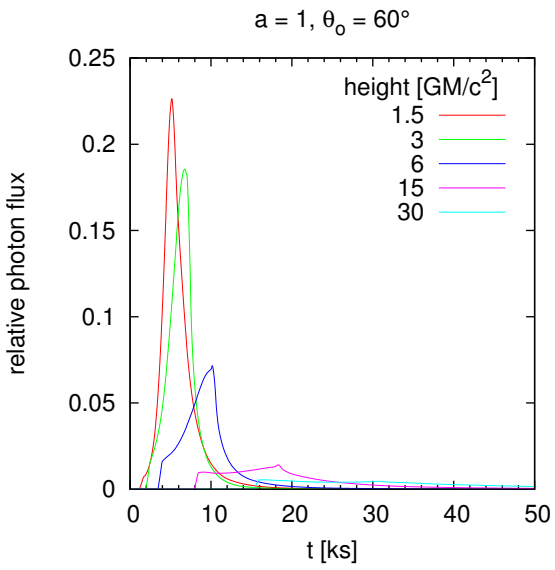

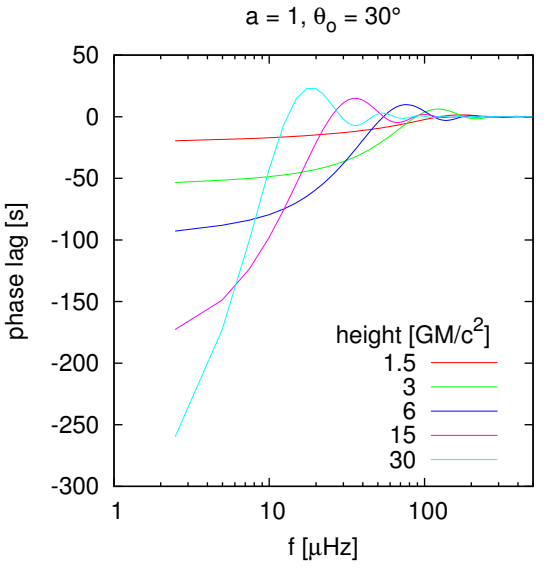

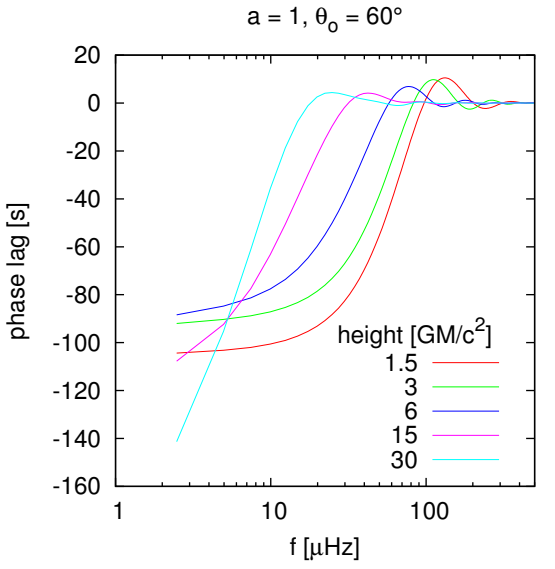

- reflected photon flux decreases with height
- primary flux increases with hight
- the delay of response is increasing with height
- the “duration” of the response is longer
- the phase lag increases with height, it depends mainly on the “average” response time and magnitude of relative photon flux
- the phase lag null points are shifted to lower frequencies for higher heights due to longer timescales of response

Phase lag dependence on geometry

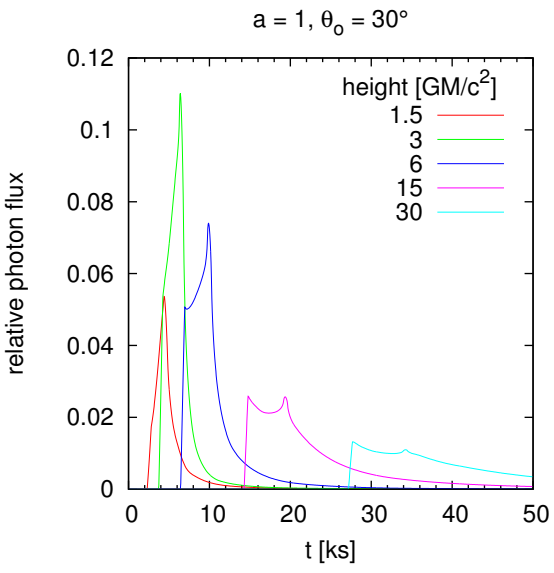

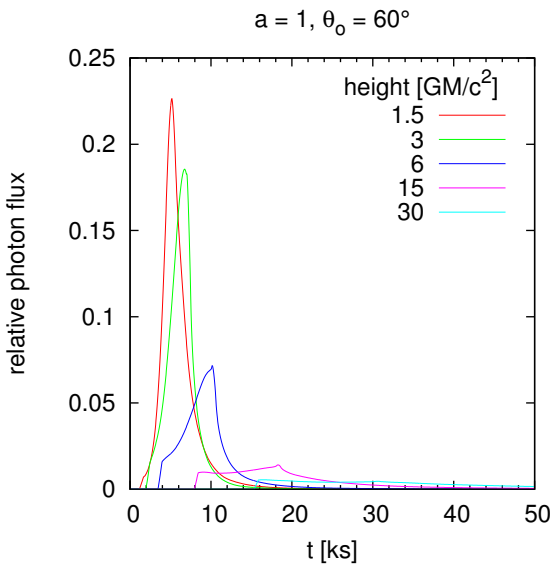

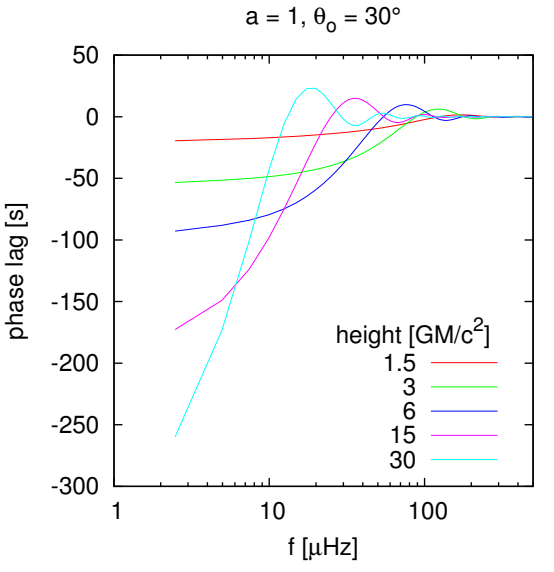

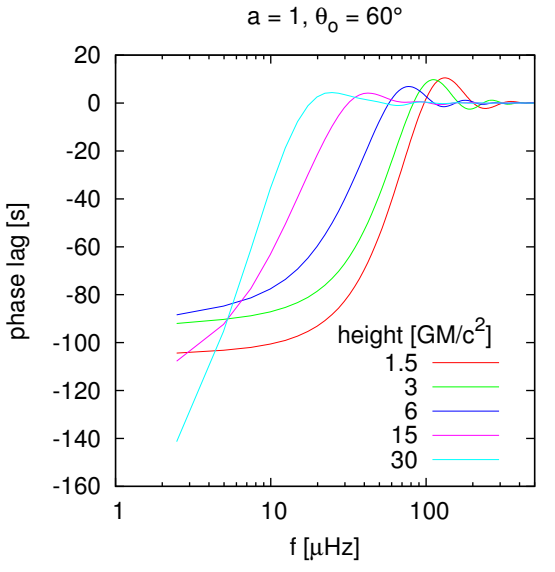

- relative photon flux and the phase lag increase with inclination for low heights
- the delay and duration of response do not change much with the inclination and thus the phase lag null points frequencies change only slightly

Phase lag dependence on spin and energy band

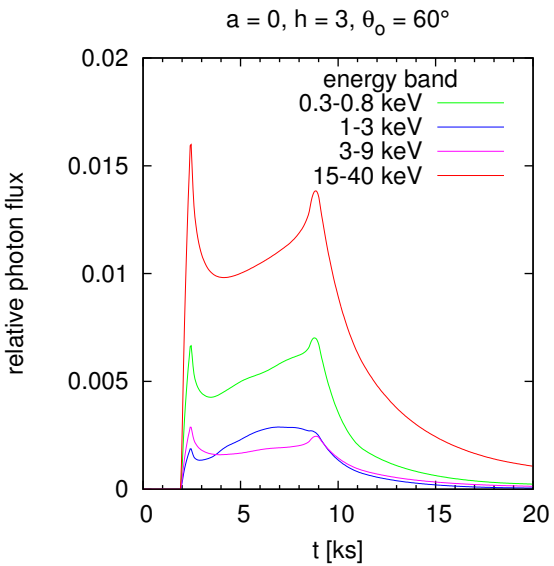

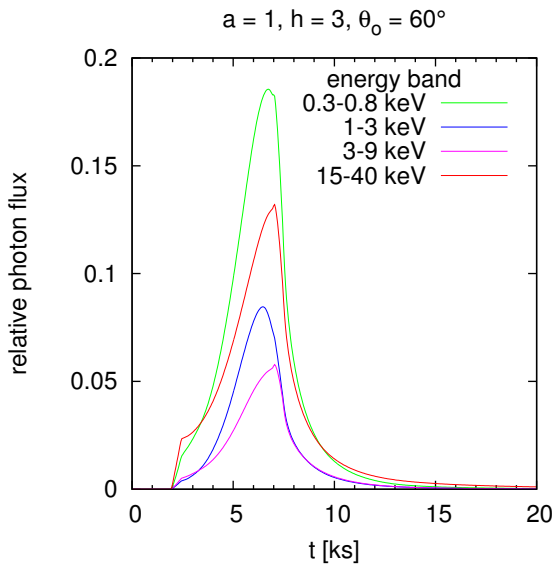

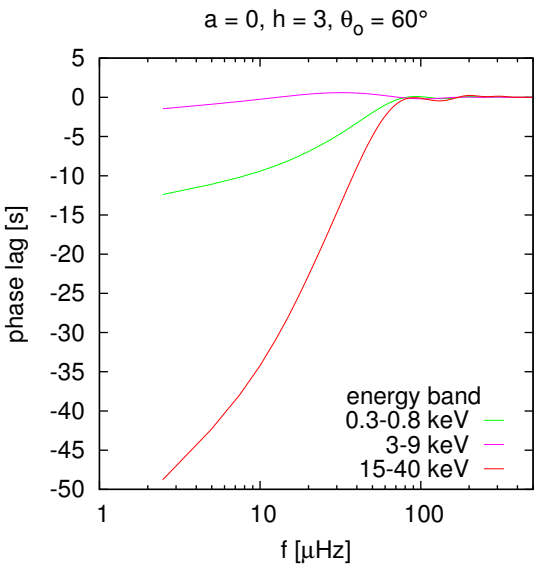

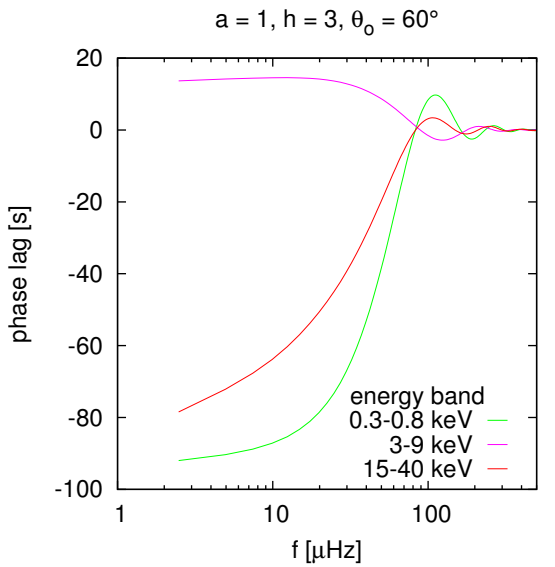

- the relative flux in the energy band where primary dominates may in some cases be larger than that in Kα and Compton hump energy bands
- the magnitude of the phase lag in different energy bands differs (in extreme Kerr case the larger lag in SE is due to larger ionisation near BH)
- the magnitude of the phase lag is smaller in Schwarzschild case due to the hole in the disc under the ISCO
- the null points of the phase lag change only slightly with energy and spin

Ionisation

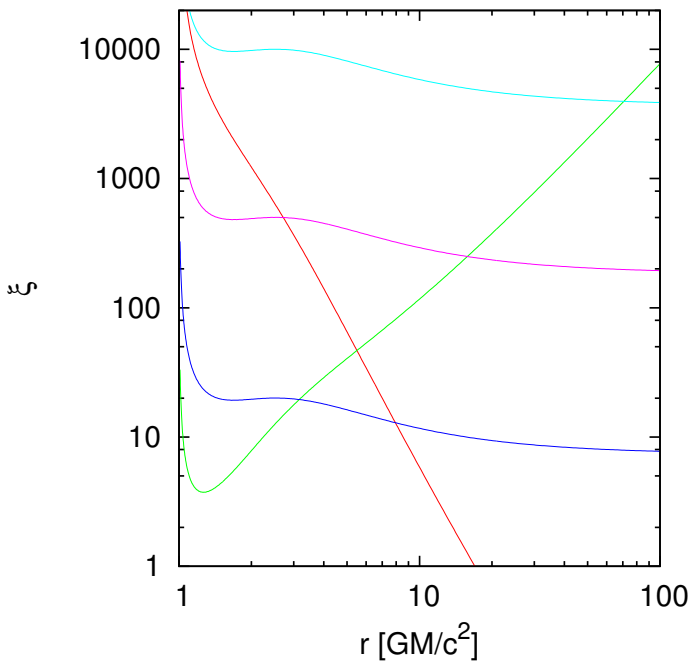

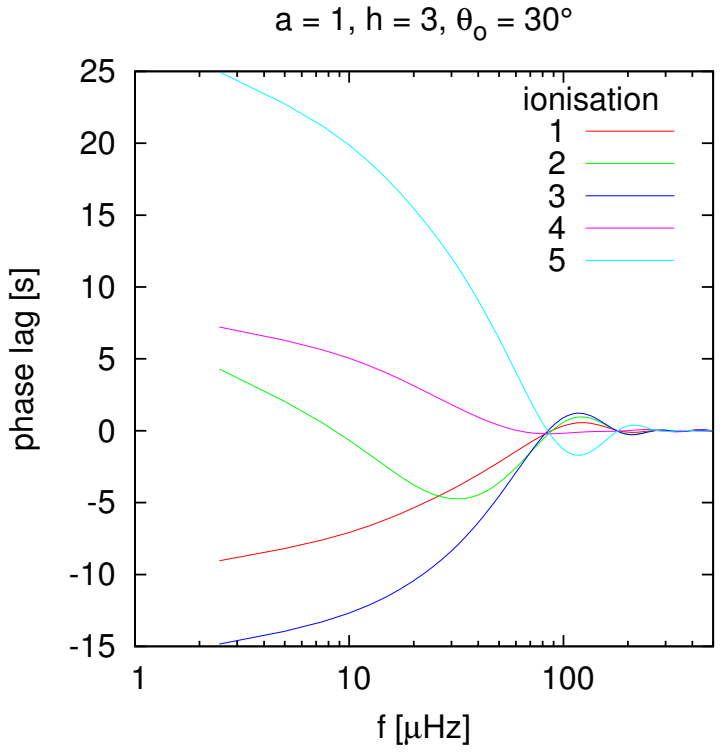

- the phase lag in Kα band is shown
- the reflection component of the spectra are steeper for higher ionisation
- the magnitude of the phase lag depend on ionisation
- the null points of the phase lag does not change with the ionisation

Directionality and photon index

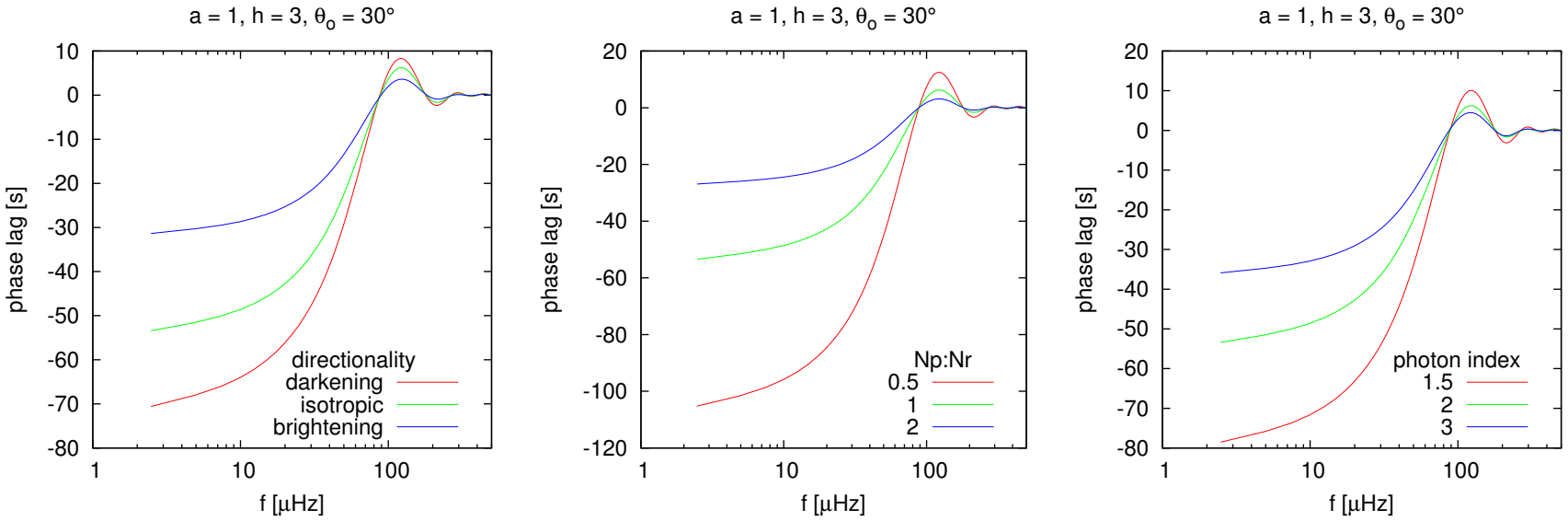

- the phase lag in SE band is shown
- the magnitude of the phase lag changes in all three cases
- the null points of the phase lag does not change with different directionility dependences or power-law photon index

Phase lag energy dependence

for low f:

$$\begin{aligned} A_{\mathrm{r}}(E,f) &\simeq A_{\mathrm{E}}(E)A_{\mathrm{f}}(f) \\ \phi_{\mathrm{r}}(E,f) &\simeq \phi_{\mathrm{r}}(f) \end{aligned}$$

and

$$\Delta\tau(E,f) \simeq \frac{1}{2\pi f}\,\mathrm{atan}\,\frac{[A_{\mathrm{r}}(E,f)-A_{\mathrm{r}}(E_0,f)]\sin\phi_{\mathrm{r}}(f)}{1+[A_{\mathrm{r}}(E,f)+A_{\mathrm{r}}(E_0,f)]\cos\phi_{\mathrm{r}}(f)+A_{\mathrm{r}}(E,f)A_{\mathrm{r}}(E_0,f)}$$

and for f such that $\phi_{\mathrm{r}}(f) = \pm\frac{\pi}{2}$:

$$\Delta\tau(E,f) \simeq \frac{1}{2\pi f}\,[A_{\mathrm{r}}(E,f)-A_{\mathrm{r}}(E_0,f)]$$

Phase lag energy dependence

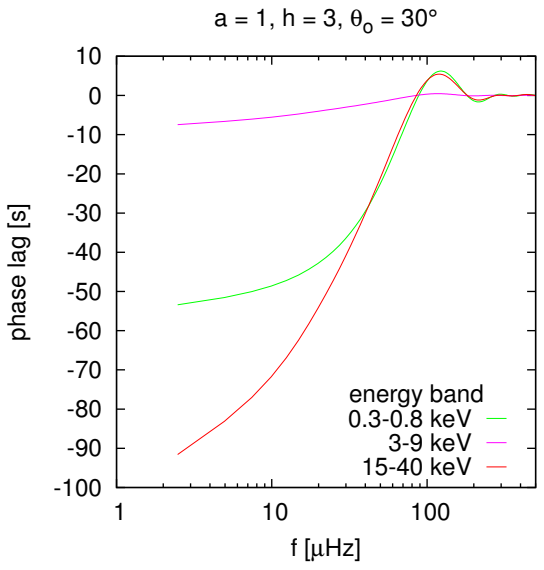

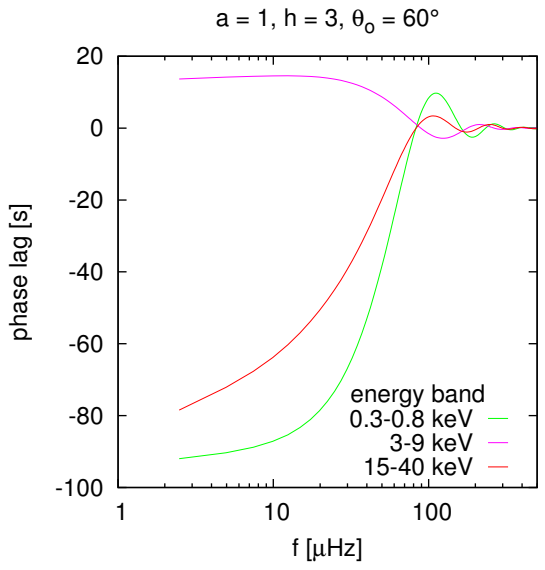

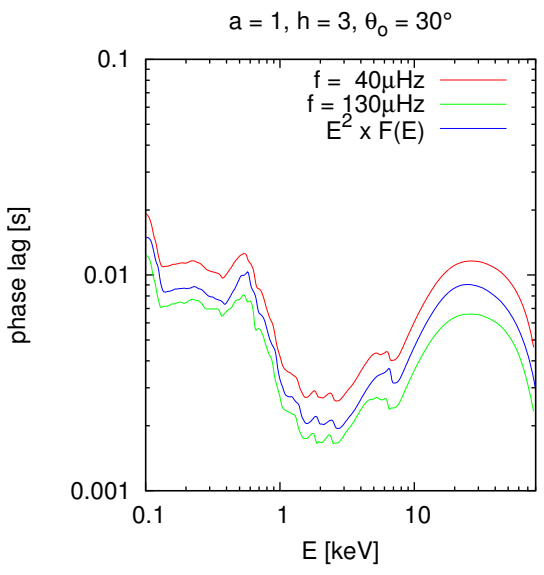

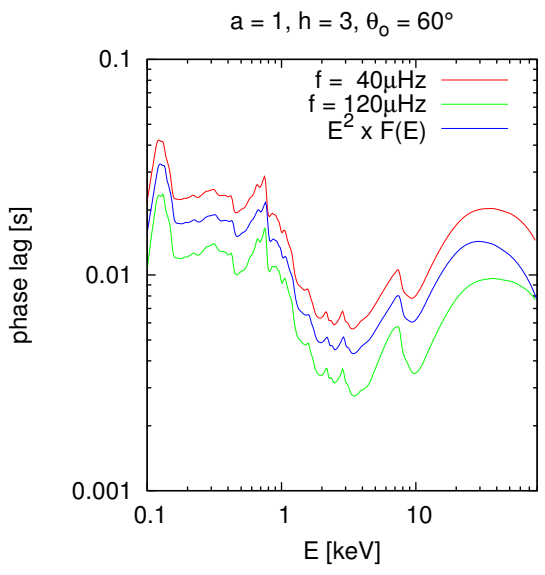

- the energy dependence of the phase lag follows the spectral shape perfectly at particular frequencies

Phase lag energy dependence

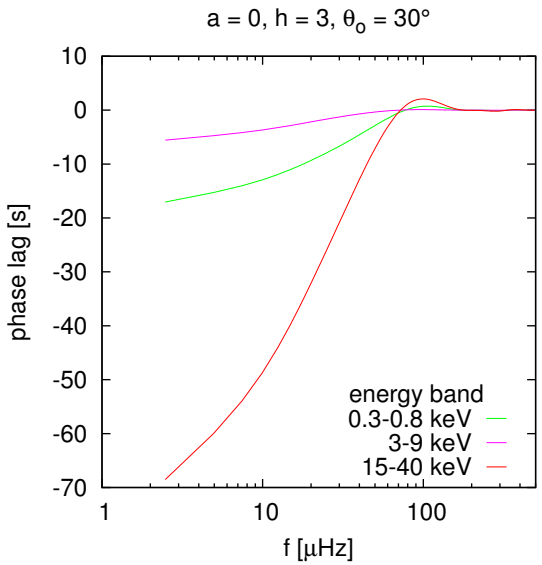

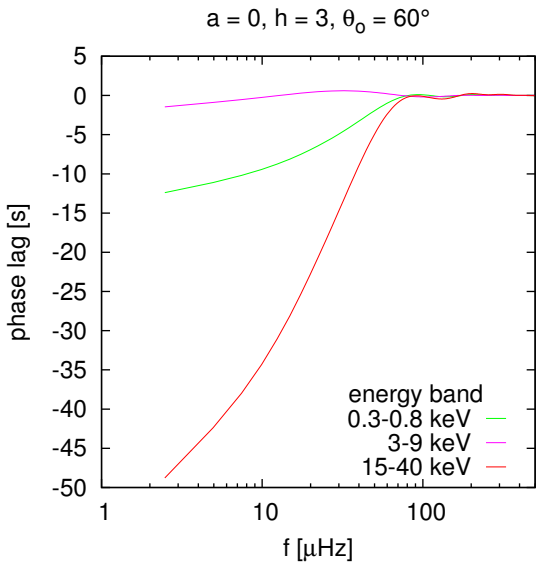

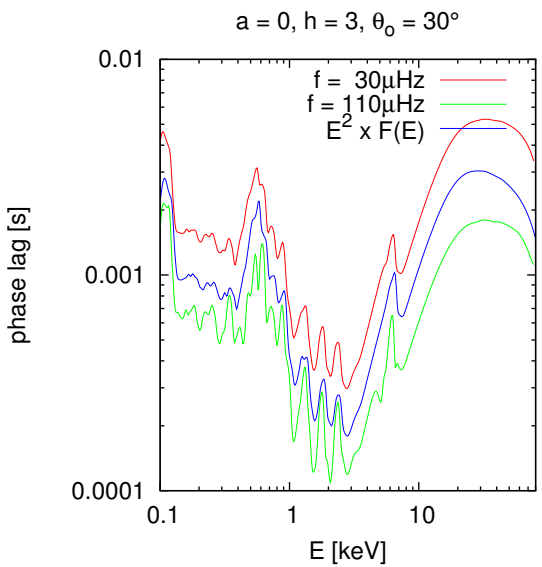

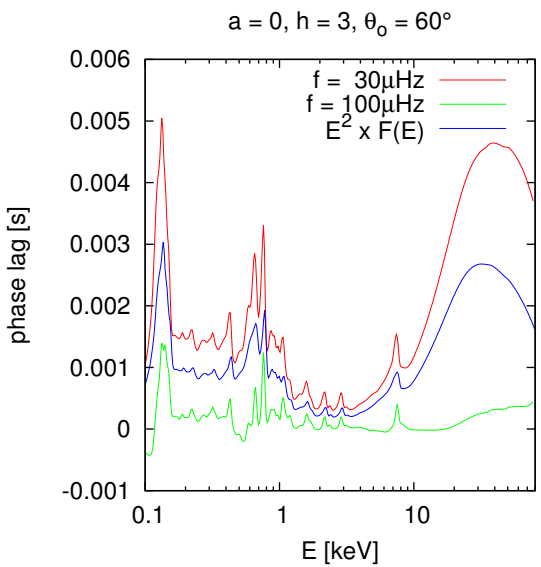

- if the second phase lag maximum is too small the phase lag energy dependence does not follow the spectral shape that well

Summary

- two aspects of reverberation – in the timing and frequency domains
- the response of the disc peaks in the vicinity of the black hole
- the phase lag is used to get information on the system properties
- the frequency dependence of the phase lag is mainly due to geometry (height of the corona)
- the magnitude of the phase lag depends on many details of the model (height, spin, ionisation, unisotropy, energy, ...)
- extended corona
  $\rightarrow$ brings several new parameters
  (size, propagation speed, “ignition” position, inhomogeinities)
  $\rightarrow$ broadens the response of the disc